AGU PUBLICATIONS

JGR

Journal of Geophysical Research: Atmospheres

RESEARCH ARTICLE
10.1002/2016JD025033

The influence of ozone forcing on blocking in the Southern Hemisphere

Fraser W. Dennison[1,2], Adrian McDonald[1], and Olaf Morgenstern[2]

[1]Department of Physics and Astronomy, University of Canterbury, Christchurch, New Zealand, [2]Now at National Institute of Water and Atmospheric Research, Wellington, New Zealand

Key Points:
- Blocking in the Atlantic region increases as a result of ozone depletion
- No change in blocking related to ozone depletion is found in the Pacific region
- Changes in blocking frequency is linked to response to the statospheric SAM index

Correspondence to:
F. W. Dennison,
fraser.dennison@niwa.co.nz

Citation:
Dennison, F. W., A. J. McDonald, and O. Morgenstern (2016), The Influence of Ozone Forcing on Blocking in the Southern Hemisphere, *J. Geophys. Res. Atmos.*, *121*, 14,358–14,371, doi:10.1002/2016JD025033.

Received 3 MAR 2016
Accepted 30 NOV 2016
Accepted article online 9 DEC 2016
Published online 20 DEC 2016

Abstract We investigate the influence of ozone depletion and recovery on tropospheric blocking in the Southern Hemisphere. Blocking events are identified using a persistent positive anomaly method applied to 500 hPa geopotential height. Using the National Institute for Water and Atmospheric Research-United Kingdom Chemistry and Aerosols chemistry-climate model, we compare reference runs that include forcing due to greenhouse gases (GHGs) and ozone-depleting substances to sensitivity simulations in which ozone-depleting substances are fixed at their 1960 abundances and other sensitivity simulations with GHGs fixed at their 1960 abundances. Blocking events in the South Atlantic are shown to follow stratospheric positive anomalies in the Southern Annular Mode (SAM) index; this is not the case for South Pacific blocking events. This relationship means that summer ozone depletion, and corresponding positive SAM anomalies, leads to an increased frequency of blocking in the South Atlantic while having little effect in the South Pacific. Similarly, ozone recovery, having the opposite effect on the SAM, leads to a decline in blocking frequency in the South Atlantic, although this may be somewhat counteracted by the effect of increasing GHGs.

1. Introduction

Atmospheric blocking refers to large, quasi-stationary, high-pressure features that persist beyond the synoptic timescale and inhibit the midlatitude zonal flow. Most of the blocking in the Southern Hemisphere occurs in the South Pacific region and, to a lesser extent, the southwestern Atlantic and exhibits a strong seasonal cycle with blocking being more common during winter and autumn [*Trenberth and Mo*, 1985; *Sinclair*, 1996; *Renwick*, 2005]. Blocking has been shown to have significant effects on the weather over midlatitude continental regions. South Atlantic blocking events result in colder conditions over much of Argentina and warmer conditions on the southern tip of the South American continent and the Antarctic Peninsula [*Mendes et al.*, 2008]. *Kayano* [1999] found that blocking over the East Pacific during summer results in colder, drier conditions in South America south of 40°S. Blocking in the Oceania region was found to produce significantly colder conditions in Southern Australia [*Mendes et al.*, 2008]. The amount of rainfall in Southern Australia is also influenced by blocking with the direction of influence determined by the location of the blocking event [*Risbey et al.*, 2009; *Cowan et al.*, 2013; *Pook et al.*, 2013]. Blocking also plays a role in the Australian heat waves [*Pezza et al.*, 2012].

There is no universally accepted metric with which to diagnose blocking; generally, the methods used are variations on two approaches. One is based on the work of *Rex* [1950] which takes reversals in the meridional geopotential height (GPH) or potential temperature gradient as indications of blocking [*Lejenäs and Økland*, 1983; *Tibaldi and Molteni*, 1990; *Pelly and Hoskins*, 2003]. The other looks for persistent positive anomalies (PPAs) in either surface pressure or GPH fields [*Dole and Gordon*, 1983; *Renwick*, 2005; *Parsons et al.*, 2016]. In comparing the two approaches, *Liu* [1994] found that PPAs centered around 60°N correspond well with the *Rex* [1950] definition of blocking, but not as well for PPAs centered around 45°N. In this study we use the PPA approach.

Large-scale modes of variability such as the El Niño–Southern Oscillation (ENSO) and Southern Annular Mode (SAM) are known to have an effect on blocking in the Southern Hemisphere. *Oliveira et al.* [2014] showed that the El Niño conditions had the effect of increasing the number of blocked days over the central and eastern Pacific, while La Niña conditions decrease the number of blocked days over the western and central Pacific.

Mendes and Cavalcanti [2014] found that blocking in the West Pacific and Atlantic regions is more frequent when the SAM is positive and more frequent in the southeast Pacific when the SAM is negative. The interplay between the ENSO and SAM is also significant [*Oliveira et al.*, 2014].

In this paper we investigate the influence of ozone depletion and recovery on blocking in the Southern Hemisphere. To reveal the effect of ozone forcing, we use a coupled atmosphere-ocean chemistry-climate model (AOCCM) which produces simulations in which ozone-depleting substances (ODSs) are either prescribed according to historical and projected concentrations or held fixed. Further information on the model and data analysis procedures is contained in section 2. In section 3 we assess the model simulation of atmospheric blocking by comparison with reanalysis data and also illustrate the effect of ozone forcing on blocking, with particular regard to how this varies by region. Section 4 includes a discussion of the mechanisms behind the relationship between ozone forcing and blocking as well as a summary of the results. The appendix provides some additional validation of the model.

2. Data and Methods

2.1. Model

The model used in this study is the National Institute for Water and Atmospheric Research-United Kingdom Chemistry and Aerosols (NIWA-UKCA) coupled atmosphere-ocean chemistry-climate model (AOCCM). The model consists of an early, low-resolution version of the Hadley Centre Global Environment Model version 3 atmosphere-ocean (HadGEM3-AO) atmosphere model, which includes the Nucleus for European Modelling of the Ocean model and the Los Alamos sea ice model (CICE), and the NIWA-UKCA chemistry module [*Hewitt et al.*, 2011; *Morgenstern et al.*, 2009]. Our reference simulation has greenhouse gases (GHGs) following the Representative Concentration Pathway 6.0 (RCP6.0) scenario [*Meinshausen et al.*, 2011] and chlorinated or brominated ozone-depleting substances (ODSs) following the A1 scenario [*WMO*, 2011]. The A1 scenario assumes continued compliance with the Montreal protocol. This simulation is referred to as "REF-C2" [*Eyring et al.*, 2013] and covers 1950–2100; there are five runs of this scenario. To isolate the effect of ozone depletion, the REF-C2 ensemble will be compared to a second smaller ensemble of two SEN-C2-fODS simulations [*Eyring et al.*, 2013]; these runs differ from REF-C2 only in that ODSs are held fixed at their 1960 levels, thereby removing the impacts of ozone depletion. Similarly, the effect of GHG forcing is isolated by comparing the REF-C2 runs to a third ensemble consisting of three runs, SEN-C2-fGHG, in which GHGs are held constant at 1960 levels. These sensitivity simulations are initialized from two or three REF-C2 simulations, respectively, and cover the period 1960–2100. These simulations have been used in other studies such as *Morgenstern et al.* [2014], *Dennison et al.* [2015], and *Oberländer-Hayn et al.* [2016].

We compare the model output to the European Centre for Medium-Range Weather Forecasts Interim Reanalysis (ERA-Interim) [*Dee et al.*, 2011]. ERA-Interim assimilates meteorological and ozone measurements from a variety of sources; the ozone product has been shown to be consistent with independent satellite measurements [*Dragani*, 2011].

2.2. Blocking Metric

Blocking is examined using the persistent positive anomaly (PPA) approach [*Renwick*, 2005]. A grid point is defined as blocked if an anomaly of greater than 100 m in the 500 hPa GPH persists for five or more days. The blocking frequency is the percentage of days for which this criterion is met over a given time frame. This technique allows blocking to be examined on a regional basis. In this paper we consider two regions, namely, the Pacific (120°W to 180°W and 42.5°S to 60°S) and Atlantic (45°W to 15°E and 42.5°S to 60°S). We define these regions as "blocked" if the number of grid points within the geographic limits described above exceeds a threshold and "not blocked" if none of the grid points fit the definition. The threshold for model data is 20 (of 102) grid points, for the reanalysis (which has a higher longitudinal resolution relative to the model) the threshold is 30 (of 150) grid points.

2.3. SAM calculation

The Southern Annular Mode (SAM) index is calculated from zonal mean GPH anomalies using an empirical orthogonal function (EOF) method. GPH anomalies are calculated relative to a slowly varying mean such that ozone depletion and recovery have no effect on the mean state of the SAM. Full details of the calculation can be found in *Dennison et al.* [2015].

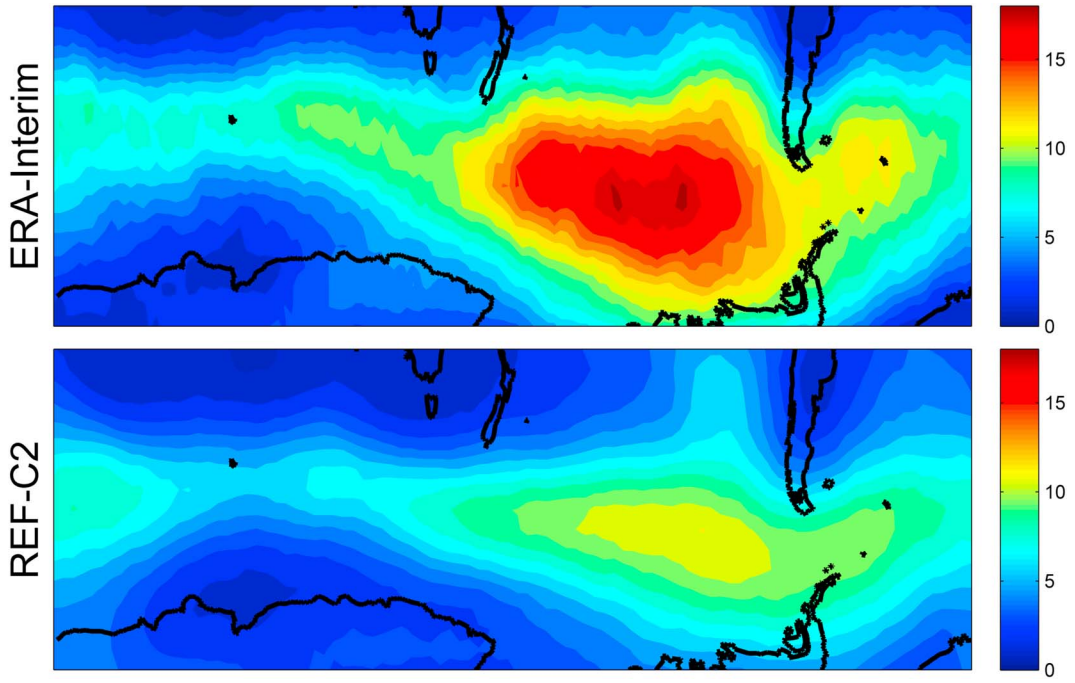

Figure 1. Annual mean blocking frequency in (top) ERA-Interim and (bottom) REF-C2 over the period 1979–2014.

3. Results

In order to validate the model we examine the annual mean blocking frequency for the period 1979–2014, shown in Figure 1 for both the ERA-Interim reanalysis (top) and the REF-C2 ensemble (bottom). The model does well in simulating the spatial pattern, correctly positioning the maxima in blocking frequency in the eastern Pacific sector and the minima in the Indian Ocean sector. The spatial correlation between these patterns is 0.88. However, the model underestimates the magnitude of the blocking frequency by around a third. Underestimation of the blocking frequency is a common problem among climate models [*D'Andrea et al.*, 1998; *Scaife et al.*, 2010]; this is discussed further in section 4.

We now examine the seasonal cycle of blocking and the effect on blocking of ozone depletion. In order to highlight the effect of ozone depletion, we initially examine the period 1987–2036 which corresponds to the period of maximum ozone depletion as simulated by the model. During this period the October- and

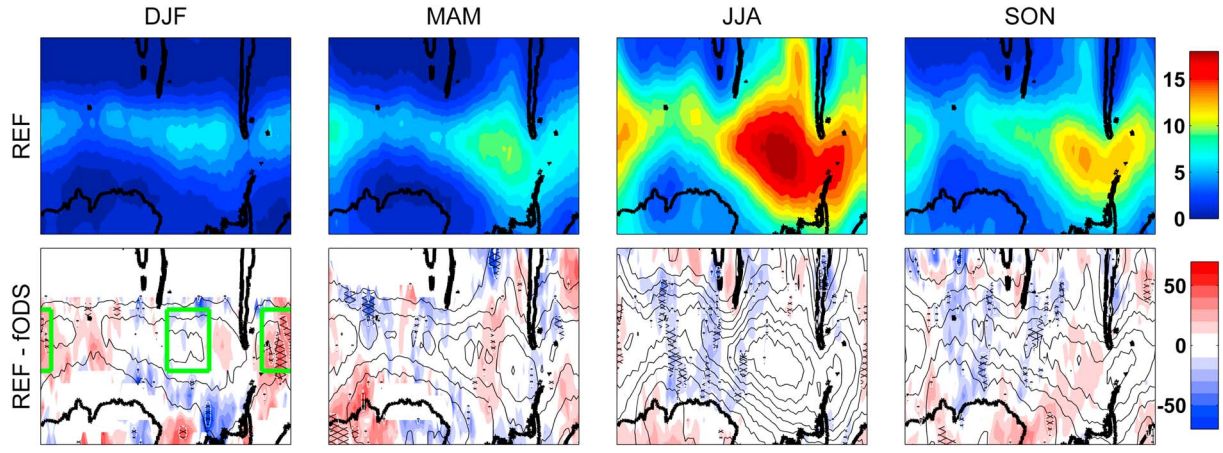

Figure 2. Seasonal mean blocking frequencies for (top row) REF-C2 and the percentage difference between (bottom row) REF-C2 and SEN-C2-fODS (shading) over the period 1987–2036; hatching indicates the difference exceeds two standard deviations. The mean blocking frequency of SEN-C2-fODS is also illustrated in Figure 2 (bottom row) in contours (increments of 2% beginning at 2%). The green boxes indicate the Pacific and Atlantic regions referenced throughout this paper.

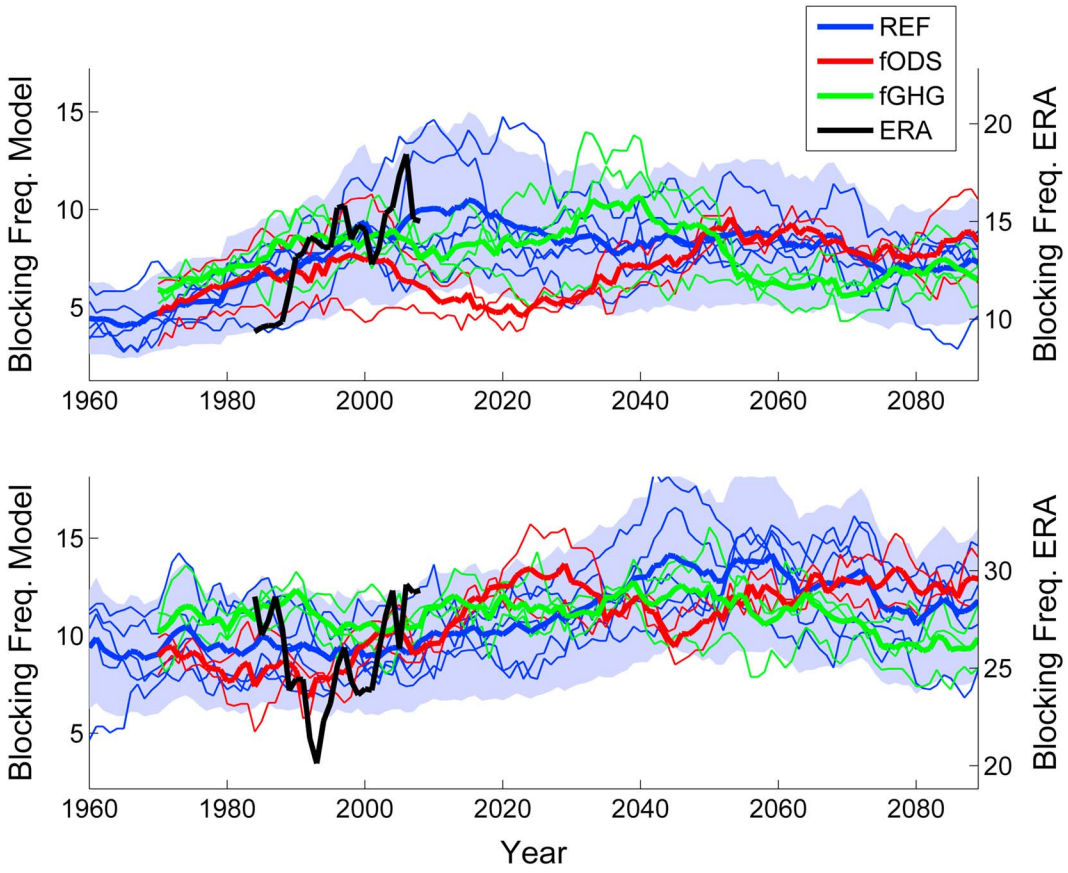

Figure 3. Time series of the summer blocking frequency in the (top) Atlantic and (bottom) Pacific in each of the model simulations REF-C2 (blue), SEN-C2-fODS (red), SEN-C2-fGHG (green), and the ERA-Interim reanalysis (black). Thin lines show the individual model runs, thick lines show the ensemble mean, and the shading indicates the 95% confidence interval around the REF-C2 ensemble mean. Note that the model and ERA–Interim reanalysis use different scales on the vertical axis to aid comparison.

areal-mean total column ozone south of 70°S is less than 220 DU (see Figure A1 in Appendix A). The top row of Figure 2 shows the seasonal blocking frequencies in the REF-C2 runs. There is a large seasonal cycle with blocking more frequent during the winter season. This seasonal cycle is consistent with other studies [e.g., *Renwick*, 2005; *Mendes et al.*, 2008; *Parsons et al.*, 2016]. Figure 2 (bottom row) illustrates the effect of ozone depletion by showing the differences between the REF-C2 and SEN-C2-fODS ensembles in each season. The differences are presented as percentage changes relative to the REF-C2 blocking frequency. For example, if the blocking frequency in the REF-C2 ensemble is 6% and in SEN-C2-fODS it is 4%, then the difference is +33%. Significant differences are marked with cross-hatching. Differences are considered significant if the difference in the ensemble means exceeds twice the REF-C2 intraensemble standard deviation. This analysis shows two instances where ozone depletion appears to have affected the blocking frequency: (1) In the South Atlantic in summer blocking appears to have increased as a result of ozone depletion. (2) In the southern Indian Ocean in winter (and to a lesser extent in spring) blocking has decreased. The South Atlantic effect is the larger of the two, and our a priori expectation is that ozone depletion generally affects the summer season [*Thompson et al.*, 2011]. For these reasons we will focus on the Atlantic region during summer. In contrast to the South Atlantic, modeled blocking in the South Pacific is not affected by ozone depletion. By contrasting these two regions we will investigate the reasons behind the change in the Atlantic region. The regions are highlighted in Figure 2.

Figure 3 shows the time series of the summer blocking frequency over the Atlantic and Pacific regions for the three scenarios and the ERA-Interim reanalysis. The shaded region around the REF-C2 ensemble illustrates the 95% confidence interval; this was estimated based on the deviations of individual runs with respect to the ensemble mean and assumes the variance is proportional to the magnitude of the blocking frequency

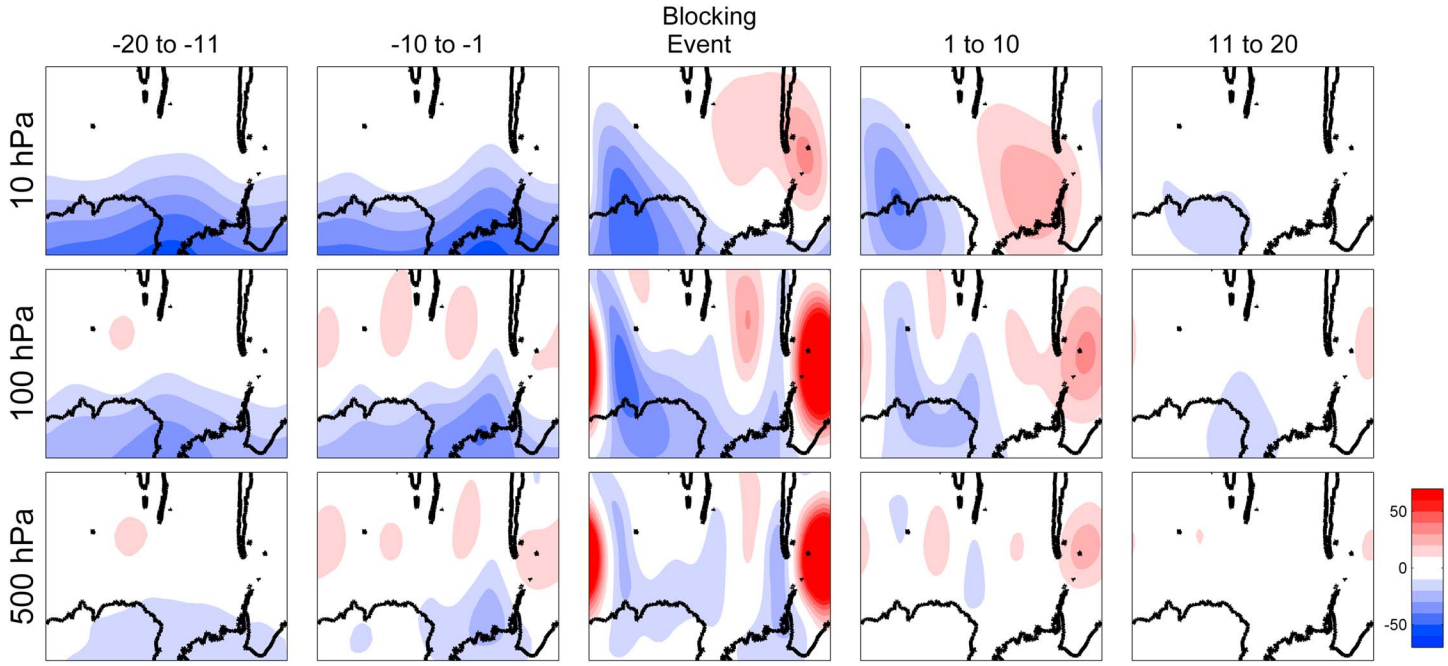

Figure 4. GPH anomalies (left to right) prior to, during, and following summer blocking events in the Atlantic at pressure levels (top row) 10, (middle row) 100, and (bottom) 500 hPa for the REF-C2 runs over the period 1950–2099. All colored anomalies are significant ($p < 0.05$) according to Wilcoxon's signed rank test.

and does not otherwise vary as a function of time. The time series of the REF-C2 and SEN-C2-fODS ensembles confirm that the difference between the two in the Atlantic that was shown in Figure 2 is confined to the ozone depletion period. The ensemble means begin to diverge during the late 1990s and converge around 2050 while closely tracking each other at the beginning and end of the simulation. The SEN-C2-fODS ensemble lies outside the bounds of the REF-C2 confidence interval over the period 2010–2025.

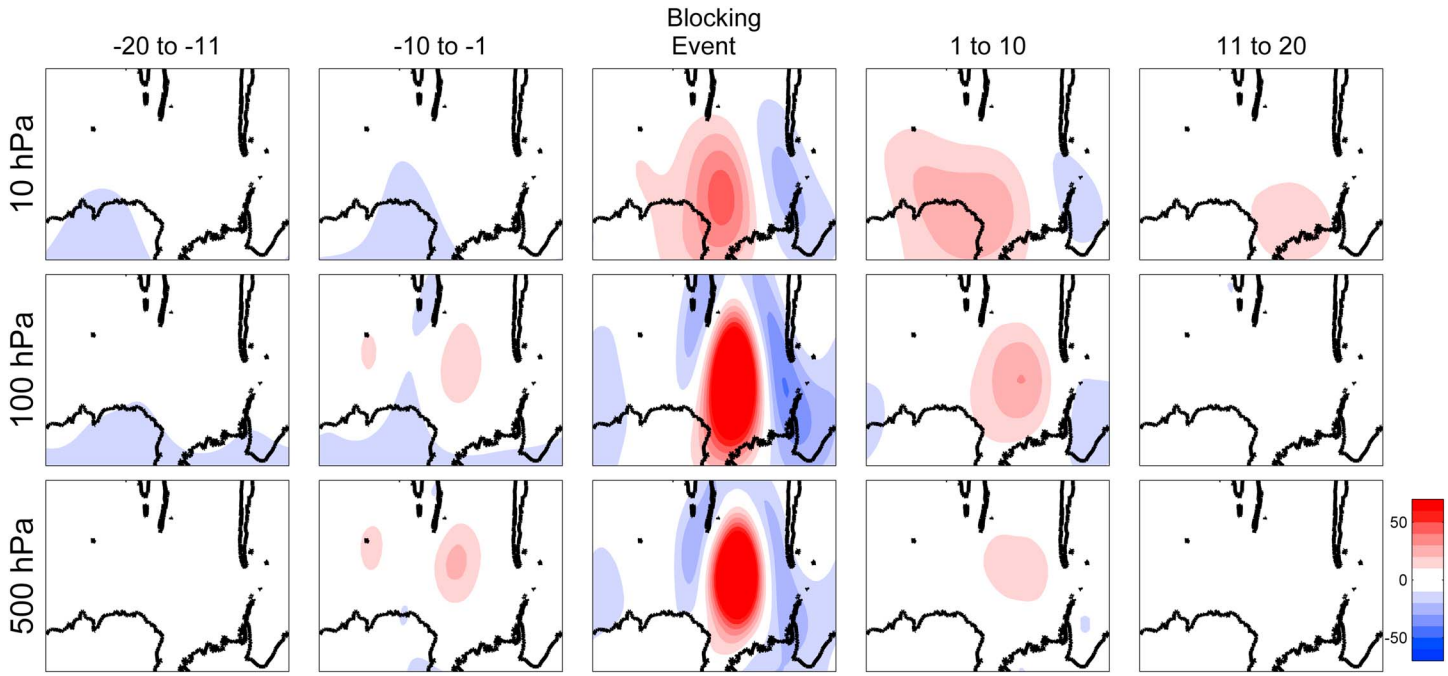

Figure 5. As for Figure 4 with Pacific blocking.

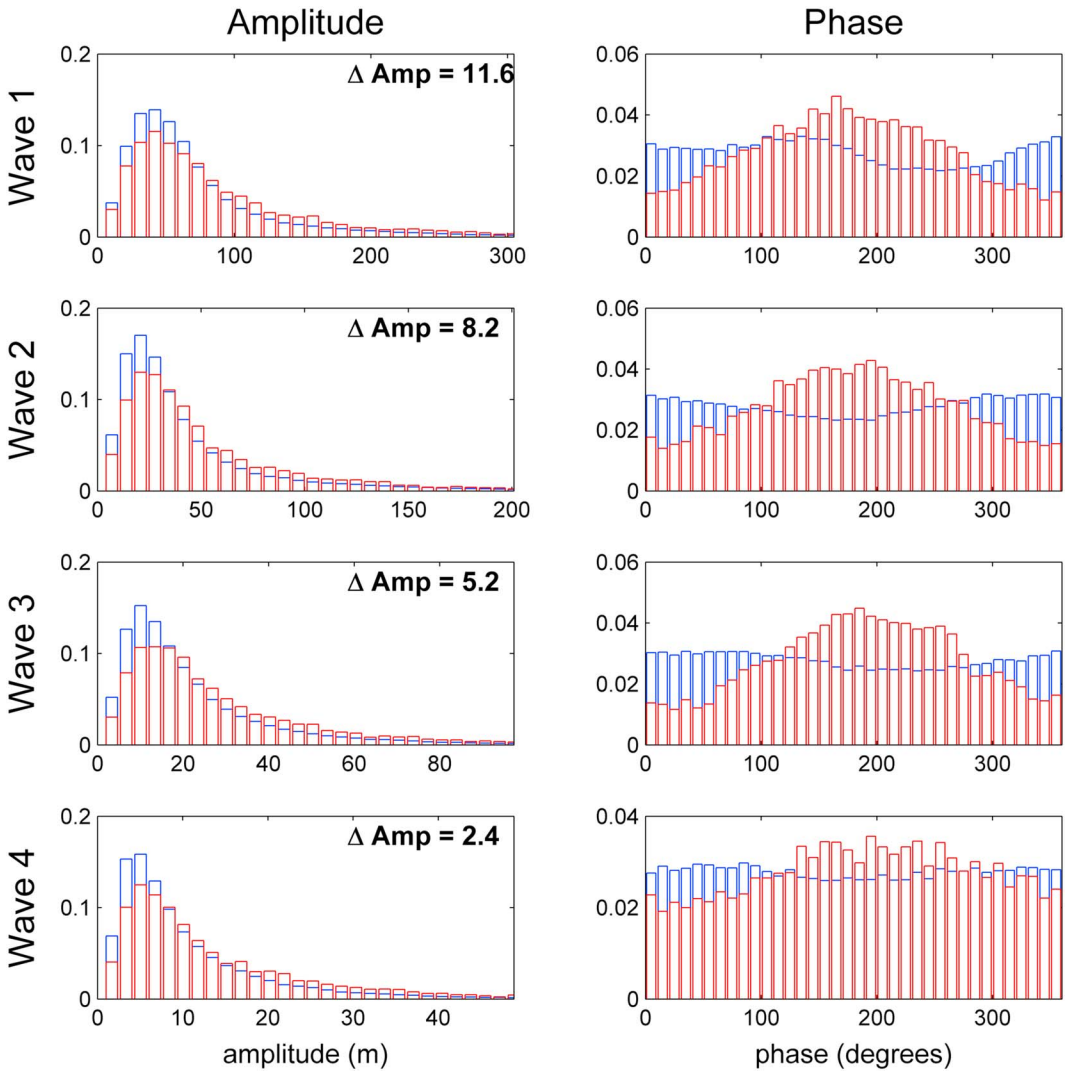

Figure 6. Probability density functions (PDFs) of the (left) amplitude and (right) phase of the first four wave components at 10 hPa during summer blocking events (red) and without blocking (blue) in the Atlantic over the period 1950–2099. ΔAmp notes the difference in medians and is bold if the difference is significant ($p < 0.05$).

As was indicated in Figure 1, the blocking frequency calculated for the ERA-Interim data set is larger than the model. To aid comparison, we therefore use different vertical scales for the model and ERA-Interim output in Figure 3. The ERA-Interim trends in blocking frequency in each of the regions match the modeled trends, namely, a positive trend in the South Atlantic and no significant trend in the South Pacific. For the South Atlantic region, the trend in ERA-Interim is larger than the mean REF-C2 one, although Figure 3 indicates that there is substantial variability among the ensemble members with two of the five REF-C2 runs exhibiting trends of magnitudes similar to the ERA-Interim trend. Also, if the trends are expressed relative to the mean blocking frequency, then there is no significant disagreement with a 16.5%/decade trend (relative to the 1979–2014 mean blocking frequency) for the REF-C2 ensemble ($p = 0.076$) and 18.9%/decade trend for ERA-Interim ($p = 0.137$).

Notably, the REF-C2 time series for the Atlantic blocking has two clear trends, increasing up until about 2010 with a slower decrease thereafter. The timing of this change might be expected from an ozone-driven effect as ozone depletion peaks at around that time before slowly recovering over the remainder of the 21st century. A similar pattern is also observed for the fGHG time series although the turning point is less clear due to substantial variability and the smaller ensemble size. In contrast to the Atlantic, the Pacific region shows no significant differences between the REF-C2 and fODS runs over the entire course of the simulations. While the fGHG ensemble shows no trend in either region, both the REF-C2 and fODS ensembles have small positive

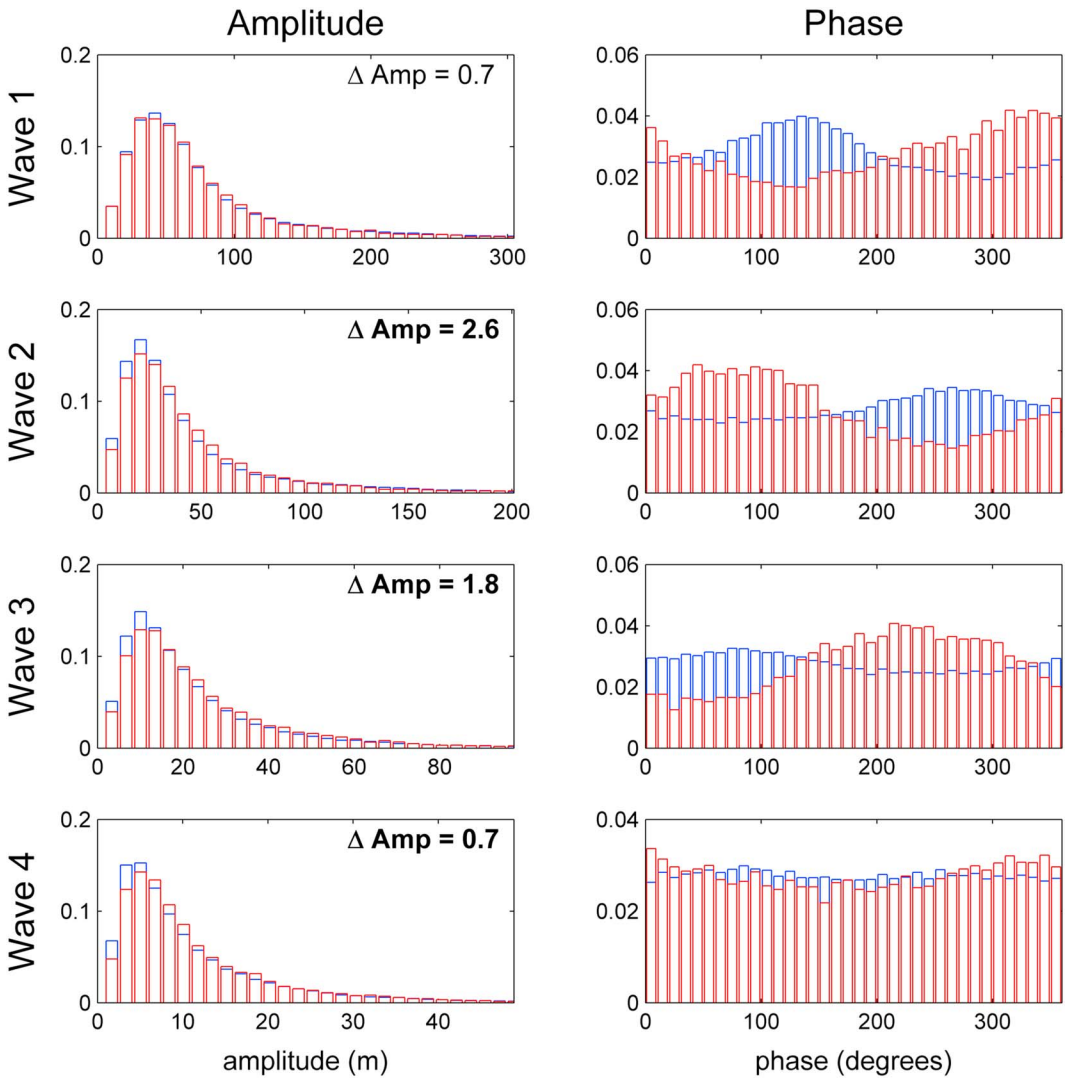

Figure 7. As for Figure 6 with Pacific blocking

trends over the duration of the simulation and exhibit a larger blocking frequency at the end of the 21st century than the fGHG runs. This suggests that increasing GHGs have the effect of increasing blocking frequency across the hemisphere. Thus, the response of blocking to ozone forcing appears to be more regional than is the case for GHG forcing.

Previous studies have suggested that the stratospheric state can impact tropospheric blocking and also that blocking can impact the stratospheric state [*Martius et al.*, 2009; *Castanheira and Barriopedro*, 2010; *Nishii et al.*, 2011; *Ayarzagüena et al.*, 2015]. This is examined in Figure 4 which shows GPH anomalies associated with summer blocking events in the Atlantic on the 10, 100, and 500 hPa pressure levels. Composites are produced for two successive 10 day periods leading up to the tropospheric blocking event, the blocking event itself, and two 10 day periods following the blocking event. The GPH is calculated relative to a slowly varying climatology in order to remove the effect of both ozone depletion and GHG forcing on the mean state. All shaded anomalies are significant ($p < 0.05$) according to Wilcoxon's signed rank test [*Wilcoxon*, 1945]. Prior to the blocking event, at 10 hPa the main feature is the negative anomaly over the polar region, i.e., a positive SAM-type pattern, which is consistent across the entire 20 day lead-up. In addition to the SAM-type pattern, there are also some small-amplitude wave 1 and 2 patterns. During the blocking event, the amplitude of the wave 1 pattern increases to become the dominant feature. The wave 1 pattern persists for the 10 days following the blocking event, then dissipates over days 11–20. Similarly, at 100 hPa the SAM-type pattern occurs prior to the blocking event. Again, the anomaly pattern characteristic of the blocking event persists in the composite of the

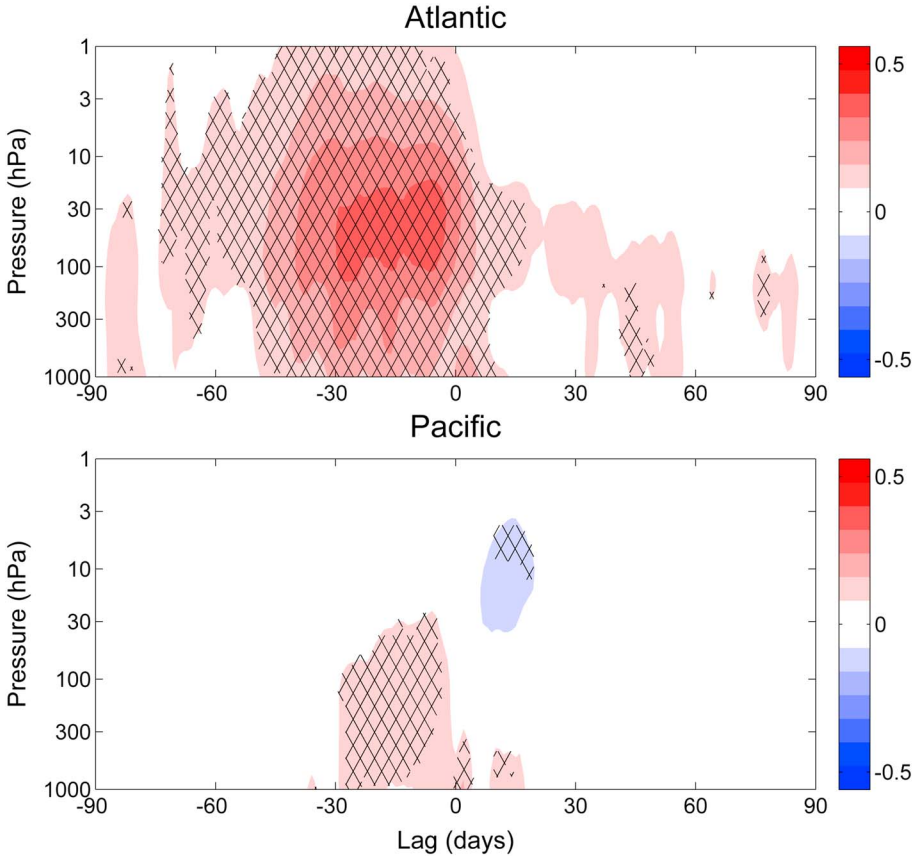

Figure 8. SAM composite of (top) Atlantic blocking and (bottom) Pacific summer blocking in the REF-C2 runs over 1950–2099. Hatching indicates significance ($p < 0.05$) according to Wilcoxon's signed rank test.

following 10 days, but it dissipates faster than at 10 hPa. The 500 hPa level does not show the same SAM feature, and in contrast to the 10 hPa level where waves 1 and 2 are more prominent, this level is dominated by waves with higher wave numbers, particularly in the periods immediately prior to and following the blocking event. Figure 5 shows the equivalent for blocking events in the Pacific. In contrast to the Atlantic, there is no sign of any SAM-type patterns, but rather just the wave 1 pattern dominating the 10 hPa level and higher wave numbers at the lower levels.

We now investigate the characteristics of the stratospheric planetary waves for the two blocking regions, as wave breaking has been shown to be a contributor to blocking [*Berrisford et al.*, 2007]. *Berrisford et al.* [2007] examine wave breaking near the tropopause; here we examine the planetary waves higher in the stratosphere where ozone depletion might be expected to have a greater influence. Figure 6 shows the probability density functions (PDFs) of the amplitude and phase of planetary waves with zonal wave numbers 1 to 4 during periods where the Atlantic region is concurrently blocked (red) or not blocked (blue), based on the criterion as defined above over the period 1950–2100. The waves components are calculated by performing a fast Fourier transform on he 55°S GPH anomaly at 10 hPa. It is clear that summer blocking is associated with waves of a certain phase, particularly for waves with zonal wave numbers 1 to 3. Interference of these waves produces the GPH anomaly shown in Figure 5 which characterizes the blocking event in the stratosphere. Also, blocking is associated with increased wave amplitude for each of the four wave components. Similarly, in the case of Pacific blocking Figure 7 shows that zonal wave numbers 1 to 3 have a clear phase preference, but there is little to no preference for an enhanced wave amplitude in this situation. The difference in median amplitude for each wave number is noted in the corner of the plot; bold font indicates that the difference in distributions is significant ($p < 0.05$) according to the Wilcoxon rank sum test [*Wilcoxon*, 1945]. It is not shown here, but a similar analysis of the 100 hPa planetary waves also shows a distinct phase preference for each wave number.

To further investigate the preference for positive SAM anomalies prior to blocking that were apparent in Figure 4, we present SAM composites showing a more detailed picture over the depth of the stratosphere and

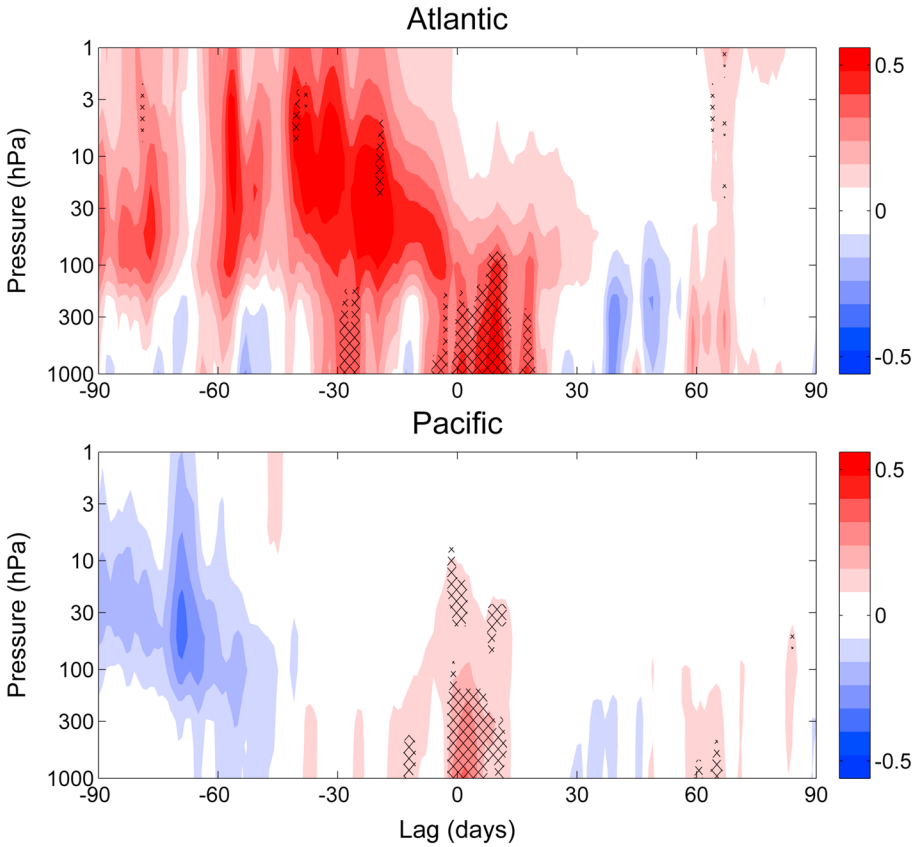

Figure 9. As for Figure 8 in the ERA-Interim reanalysis 1979–2014.

troposphere before and after the blocking event. Figure 8 (top) shows the SAM composite corresponding to blocking events in the Atlantic. Lag is relative to the onset of the blocking event; lag 0 corresponds to the first day of the blocking event. Significant SAM anomalies ($p < 0.05$) are identified by Wilcoxon's signed rank test [*Wilcoxon*, 1945] and are indicated by hatching. As Figure 4 suggested, there is a positive SAM anomaly prior to the blocking event. This anomaly lasts for 40–50 days and peaks around 30–50 hPa but extends through much of the lower stratosphere and upper troposphere. It comes to an end abruptly at the onset of the blocking event. The contrast is clear when comparing this behavior to the equivalent structure for the Pacific region shown in Figure 8 (bottom). In this case the SAM anomaly is much smaller and confined to the troposphere. Figure 9 shows the same analysis applied to the ERA-Interim reanalysis. As was the case for the model, this shows a strong positive SAM anomaly in the stratosphere preceding blocking events in the Atlantic and very little anomalous behavior associated with Pacific blocking. Note that although the stratospheric anomalies are larger for the reanalysis, they are not shown to be significant. This might be expected because the Figure 8 composite is drawn from five 150 year runs, while Figure 9 is from just 36 years, making statistical significance more difficult to obtain. A notable difference for the reanalysis is the presence of a positive SAM anomaly in the troposphere after the onset of the blocking event.

4. Discussion and Summary

The NIWA-UKCA model, when compared to the ERA-Interim reanalysis, generally simulates well many of the aspects of blocking such as the spatial distribution, seasonal cycle, and associations with the SAM. However, it underestimates the blocking frequency by around a third. This is a common problem among climate models [*D'Andrea et al.*, 1998; *Scaife et al.*, 2010], especially those with low horizontal resolution [*Anstey et al.*, 2013] (as is the case for the NIWA-UKCA model). Such models cannot simulate small-scale eddies which are important for maintaining blocking events [*Matsueda et al.*, 2009]. *Scaife et al.* [2010] also find that biases in the mean state of the model cause errors in the simulation of blocking. This may also be an issue for the NIWA-UKCA model which exhibits a poleward bias in the position of the polar front jet (see Appendix A).

Figures 2 and 3 show that ozone depletion is responsible for an increase in the frequency of blocking in the South Atlantic. This change in blocking frequency will likely have consequences for the climate of South America due to the links demonstrated by *Mendes et al.* [2008] and *Kayano* [1999] (cf. section 1). In the NIWA-UKCA simulations, the effect of ozone forcing is larger than that of GHG forcing. In the REF-C2 ensemble, the blocking frequency increases from ≈5% during the 1960s (i.e., before the onset of the ozone hole) to around 10% during the mid-2010s before recovering to around 7% toward the end of the century when GHG forcing will be the main driver of any change. Furthermore, it is also possible that the ozone depletion-driven change simulated by the model may be an underestimation of the real impact as it is shown that the rate of increase in blocking calculated from the ERA-Interim reanalysis exceeds that of the model. The ERA-Interim data cover a relatively short timespan, and given that the model simulations show considerable variability among ensemble members and on interdecadal timescales, the data at our disposal are insufficient for attributing the full increase in blocking to ozone forcing. However, we find that ozone depletion likely exerts a bigger influence on blocking in the South Atlantic during austral summer than increasing GHGs.

Another aspect of this association of ozone depletion and blocking is the demonstration of a link between stratospheric processes (i.e., a SAM anomaly at 10 hPa) and blocking, a tropospheric phenomenon. Such stratosphere-to-troposphere coupling has been demonstrated earlier regarding the NAM and SAM (respectively, *Baldwin and Dunkerton* [2001] and *Thompson et al.* [2005]). A number of subsequent studies have also investigated the links between the stratosphere and tropospheric blocking, most of which focus on Northern Hemisphere blocking. The mechanisms at work in such links are, however, not well understood.

In a somewhat analogous study of Northern Hemisphere blocking, *Woollings et al.* [2010] show that the first EOF of 10 hPa GPH (which has an annular structure) correlates with a 6 day lead with blocking in certain regions of the Northern Hemisphere. In particular, blocking over Europe was positively correlated with the phase of this EOF which described anomalously strong Arctic polar vortex conditions. However, *Yao and Luo* [2015] find that blocking events over Southern Europe follow the positive phase of the North Atlantic Oscillation (NAO+). This effect is explained simply as the high-pressure lobe of the NAO (which normally is located over the mid-Atlantic) migrating east with the enhanced westerly wind associated with the NAO+. We find that this type of mechanism, however, does not apply in the case of South Atlantic blocking because Figure 4 does not show the same large GPH anomalies prior to the blocking event.

Martius et al. [2009] examined the occurrence of sudden stratospheric warming (SSW) events in the Northern Hemisphere relative to the occurrence of blocking events building on earlier work which identified a possible two-way interplay between these phenomena. That study showed a distinct link between planetary scale waves and atmospheric blocks. For example in SSW split events they reported an almost perfect colocation between the blocking maximum in the Pacific with the positive wave number 2 wave peak at lower levels. There was also clear evidence of constructive interference of wave numbers 1 and 2 in the stratosphere resulting in the vortex split events. The current analysis (see Figure 6) also displays clear signs of synchronized wave phases during blocking in the Southern Hemisphere which would be related to constructive interference between the various planetary waves modes.

Recent work by *Davini et al.* [2014] also examined blocking in the Northern Hemisphere and its relationship to stratosphere-troposphere coupling. Their study analyzes the influence of stratospheric extremes (SSWs and also vortex intensification (VI) events) on blocking frequency and patterns in the Northern Hemisphere. The impact of the stratosphere can be summarized as a change of the blocking frequency on the flanks of the eddy-driven jet streams. Similar to the results presented in this study, *Davini et al.* [2014] find that there is a different sensitivity of the tropospheric blocking to the stratospheric forcing in the two ocean basins, with vortex anomalies leading tropospheric blocking in the Atlantic, but having no clear relationship in the Pacific. They also note a clear displacement of the Atlantic eddy-driven jet equatorward for SSWs and an opposite response for VI events. *Davini et al.* [2014] then examine one of the possible theories to explain stratosphere-troposphere coupling which involves the modulation of tropospheric synoptic waves by the lower stratospheric flow [*Kunz et al.*, 2009]. In that theory the value of the stratospheric zonal wind vertical shear determines the evolution of the baroclinic wave life cycles between two states. *Davini et al.* [2014] show, in agreement with *Kunz et al.* [2009], that the stratospheric jets impact on the zonal wind vertical shear can enhance the occurrence of Rossby wave breaking which they note is linked to blocking [*Pelly and Hoskins*, 2003].

In the case of the Southern Hemisphere various case studies [e.g., *Kodera et al.*, 2013; *Nishii and Nakamura*, 2005] have shown links between the stratosphere and tropospheric blocking. They demonstrate planetary waves of tropospheric origin either being reflected [*Kodera et al.*, 2013] or being refracted [*Nishii and Nakamura*, 2005] in the stratosphere back toward the troposphere where they result in a blocking event. These examples are taken for SH winter when westerlies are strong such that planetary wave reflection is initiated (in the *Nishii and Nakamura* [2005] case study) by an increase in the strength of the westerlies. In this case while the positive SAM anomaly is associated with increased westerlies, the strength of the westerlies during summer is not sufficient to instigate wave reflection—indeed one might expect less wave reflection due to the decreased frequency of easterlies in the stratosphere. Therefore, it seems it is not the change in zonal winds that is responsible for the change in blocking frequency here. The mechanisms identified in *Nishii and Nakamura* [2005] and *Kodera et al.* [2013] are therefore unlikely to be viable mechanisms in this case. One possible interpretation of the link between the SAM and Atlantic blocking demonstrated in Figure 8 is due to the zonally asymmetric component of the SAM. While the stratospheric SAM is mostly zonally symmetric, it also features a zonal wave 1 pattern; in the positive phase it is orientated such that the trough is located over the southeast Pacific [*Thompson and Wallace*, 2000]. Figure 4 shows that a trough in this location is present in the 10 days prior to Atlantic blocking events. This might suggest that it is the state of the planetary waves that influence the blocking frequency and the SAM modifies the planetary wave state in such a way that it influences only blocking in the Atlantic. A tendency toward a positive SAM (driven by ozone depletion [*Arblaster and Meehl*, 2006; *Karpechko et al.*, 2010; *Morgenstern et al.*, 2014]) therefore drives the increase in Atlantic blocking that we find while having little effect on blocking in the Pacific. The nature of the mechanism initiating these summer blocking events is still unclear; further investigation of wave propagation is perhaps required but is beyond the reach of this study due to limitations on the model data available.

Appendix A: Model Validation

This appendix provides a comparison between the NIWA-UKCA model and ERA-Interim reanalysis in order to identify the model characteristics and biases that may be relevant to this study. First, we examine the

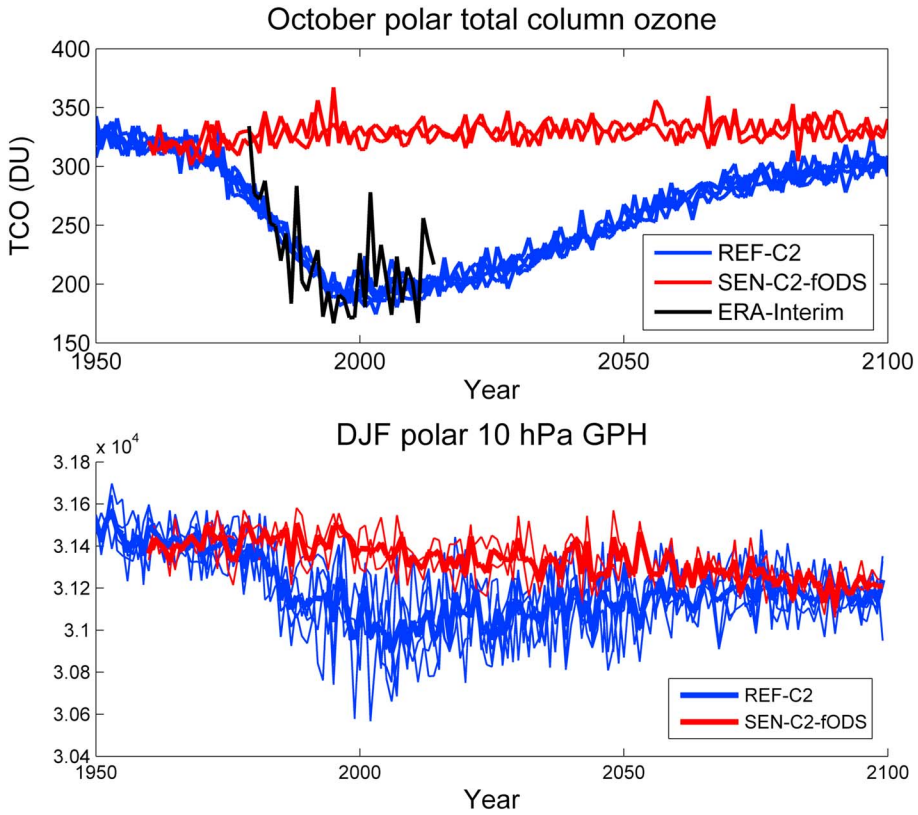

Figure A1. October mean (top) total column ozone south of 70°S and (bottom) summer 10 hPa GPH south of 80°S for REF-C2 (blue), SEN-C2-fODS (red), and ERA-Interim (black, Figure A1 (top)).

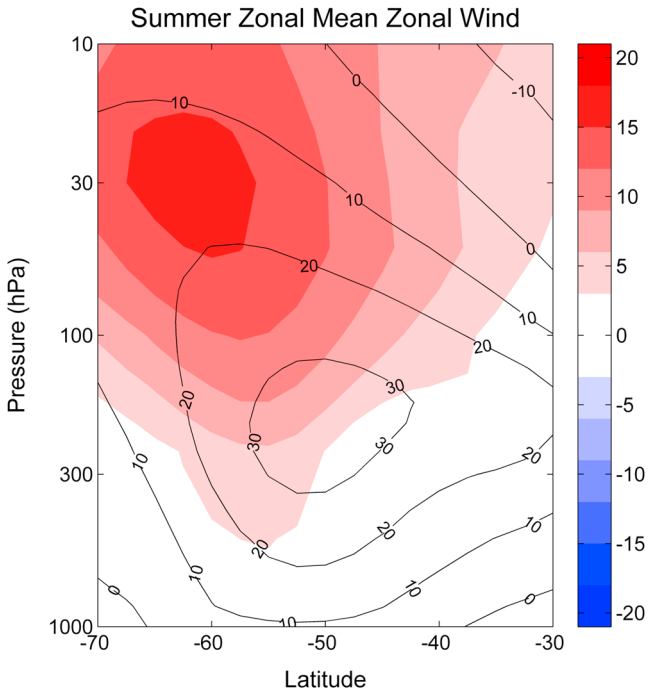

Figure A2. Summer zonal mean zonal wind for the REF-C2 runs over the period 1979–2014 (contours) and the difference between REF-C2 and the ERA-Interim reanalysis (shading).

simulated ozone depletion; Figure A1 (top) shows the October mean total column ozone south of 70°S for REF-C2 (blue) and SEN-C2-fODS (red) individual model runs compared to the ERA-Interim reanalysis (black). The REF-C2 simulates the ozone depletion trend well however seems not to capture the year to year variability (although the 2002 spike in ozone shown in ERA-Interim is due to a stratospheric sudden warming (SSW) that is not present in the model). The ozone recovery phase shows the model predicting a return to 1980 levels around the 2050s which is consistent with other chemistry-climate models [*Eyring et al.*, 2010]. This ozone depletion leads to cooling of the polar stratosphere and a decease in GPH at high latitudes. This is illustrated for the model in Figure A1 (bottom) which shows the summer mean GPH south of 80°S, where the REF-C2 (blue) and SEN-C2-fODS (red) runs are shown by thin lines and the ensemble means by thick lines. During the period of ozone depletion the REF-C2 ensemble GPH deviates from the SEN-C2-fODS ensemble by as much as 500 m. This deviation is consistent with a positive SAM anomaly.

Next we examine the mean state of the zonal winds. Figure A2 shows the difference in summer zonal mean zonal wind between the REF-C2 ensemble and ERA-Interim reanalysis over the period 1979–2014. It can be seen that model overestimates the wind strength in the polar stratosphere. This wind strength bias is present in all seasons; however, in summer the bias is exacerbated somewhat by the model tendency to delay the break-up of the polar vortex. It is possible that this bias in the mean state of the model may cause some bias in the simulation of blocking as is demonstrated in *Scaife et al.* [2010].

Acknowledgments
We acknowledge the UK MetOffice for use of the MetUM. This research has been supported by the University of Canterbury, by NIWA as part of its Government-funded, core research, and by the Marsden Fund Council from Government funding, administered by the Royal Society of New Zealand (grant 12-NIW-006). The authors wish to acknowledge the contribution of NeSI high-performance computing facilities to the results of this research. NZ's national facilities are provided by the NZ eScience Infrastructure and funded jointly by NeSI's collaborator institutions and through the Ministry of Business, Innovation and Employment's Research Infrastructure programme. The data used in the paper are available from the lead author upon request. The model output has been made available for public use via the Chemistry-Climate Model Initiative (CCMI) archive (see https://blogs.reading.ac.uk/ccmi/badc-data-access/). Data from the ERA-Interim reanalysis may be obtained from https://apps.ecmwf.int/datasets/data/interim-full-daily/.

References

Anstey, J. A., P. Davini, L. J. Gray, T. J. Woollings, N. Butchart, C. Cagnazzo, B. Christiansen, S. C. Hardiman, S. M. Osprey, and S. Yang (2013), Multi-model analysis of Northern Hemisphere winter blocking: Model biases and the role of resolution, *J. Geophys. Res. Atmos.*, *118*, 3956–3971, doi:10.1002/jgrd.50231.

Arblaster, J. M., and G. A. Meehl (2006), Contributions of external forcings to southern annular mode trends, *J. Clim.*, *19*, 2896–2905, doi:10.1175/JCLI3774.1.

Ayarzagüena, B., Y. J. Orsolini, U. Langematz, J. Abalichin, and A. Kubin (2015), The relevance of the location of blocking highs for stratospheric variability in a changing climate, *J. Clim.*, *28*(2008), 531–549, doi:10.1175/JCLI-D-14-00210.1.

Baldwin, M. P., and T. J. Dunkerton (2001), Stratospheric harbingers of anomalous weather regimes, *Science*, *294*, 581–584, doi:10.1126/science.1063315.

Berrisford, P., B. J. Hoskins, and E. Tyrlis (2007), Blocking and Rossby wave breaking on the dynamical tropopause in the Southern Hemisphere, *J. Atmos. Sci.*, *64*, 2881–2898, doi:10.1175/JAS3984.1.

Castanheira, J. M., and D. Barriopedro (2010), Dynamical connection between tropospheric blockings and stratospheric polar vortex, *Geophys. Res. Lett.*, *37*, 1–5, doi:10.1029/2010GL043819.

Cowan, T., P. Van Rensch, A. Purich, and W. Cai (2013), The association of tropical and extratropical climate modes to atmospheric blocking across southeastern Australia, *J. Clim.*, *26*, 7555–7569, doi:10.1175/JCLI-D-12-00781.1.
D'Andrea, F., et al. (1998), *Clim. Dyn.*, *14*, 385–407, doi:10.1007/s003820050230.
Davini, P., C. Cagnazzo, and J. A. Anstey (2014), A blocking view of the stratosphere-troposphere coupling, *J. Geophys. Res. Atmos.*, *119*, 100–115, doi:10.1002/2014JD021703.
Dee, D. P., et al. (2011), The ERA-Interim reanalysis: Configuration and performance of the data assimilation system, *Q. J. R. Meteorolog. Soc.*, *137*, 553–597, doi:10.1002/qj.828.
Dennison, F. W., A. J. McDonald, and O. Morgenstern (2015), The effect of ozone depletion on the Southern Annular Mode and stratosphere-troposphere coupling, *J. Geophys. Res. Atmos.*, *120*, 6305–6312, doi:10.1002/2014JD023009.
Dole, R. M., and N. D. Gordon (1983), Persistent anomalies of the extratropical Northern Hemisphere wintertime circulation: Geographical distribution and regional persistence characteristics, *Mon. Weather Rev.*, *111*, 1567–1586, doi:10.1175/1520-0493(1986)114<0178:PAOTEN>2.0.CO;2.
Dragani, R. (2011), On the quality of the ERA-Interim ozone reanalyses: Comparisons with satellite data, *Q. J. R. Meteorolog. Soc.*, *137*, 1312–1326, doi:10.1002/qj.821.
Eyring, V., et al. (2010), Multi-model assessment of stratospheric ozone return dates and ozone recovery in CCMVal-2 models, *Atmos. Chem. Phys.*, *10*, 9451–9472, doi:10.5194/acp-10-9451-2010.
Eyring, V., et al. (2013), Long-term ozone changes and associated climate impacts in CMIP5 simulations, *J. Geophys. Res. Atmos.*, *118*, 5029–5060, doi:10.1002/jgrd.50316.
Hewitt, H. T., D. Copsey, I. D. Culverwell, C. M. Harris, R. S. R. Hill, A. B. Keen, A. J. McLaren, and E. C. Hunke (2011), Design and implementation of the infrastructure of HadGEM3: The next-generation Met Office climate modelling system, *Geosci. Model Dev.*, *4*, 223–253, doi:10.5194/gmd-4-223-2011.
Karpechko, A. Y., N. P. Gillett, L. J. Gray, and M. Dall'Amico (2010), Influence of ozone recovery and greenhouse gas increases on Southern Hemisphere circulation, *J. Geophys. Res.*, *115*, 1–15, doi:10.1029/2010JD014423.
Kayano, M. (1999), Meteorology and atmospheric physics Southeastern Pacific blocking episodes and their effects on the South American weather, *Meteorol. Atmos. Phys.*, *155*, 145–155.
Kodera, K., H. Mukougawa, and A. Fujii (2013), Influence of the vertical and zonal propagation of stratospheric planetary waves on tropospheric blockings, *J. Geophys. Res. Atmos.*, *118*, 8333–8345, doi:10.1002/jgrd.50650.
Kunz, T., K. Fraedrich, and F. Lunkeit (2009), Response of idealized baroclinic wave life cycles to stratospheric flow conditions, *J. Atmos. Sci.*, *66*, 2288–2302, doi:10.1175/2009JAS2827.1.
Lejenäs, H., and H. Økland (1983), Characteristics of northern hemisphere blocking as determined from a long time series of observational data, *Tellus A*, *35*, 967–979, doi:10.3402/tellusa.v35i5.11446.
Liu, Q. (1994), On the definition and persistence of blocking, *Tellus A*, *46*, 286–298.
Martius, O., L. M. Polvani, and H. C. Davies (2009), Blocking precursors to stratospheric sudden warming events, *Geophys. Res. Lett.*, *36*, 1–5, doi:10.1029/2009GL038776.
Matsueda, M., R. Mizuta, and S. Kusunoki (2009), Future change in wintertime atmospheric blocking simulated using a 20-km-mesh atmospheric global circulation model, *J. Geophys. Res.*, *114*, 1–10, doi:10.1029/2009JD011919.
Meinshausen, M., et al. (2011), The RCP greenhouse gas concentrations and their extensions from 1765 to 2300, *Clim. Change*, *109*, 213–241, doi:10.1007/s10584-011-0156-z.
Mendes, M. C. D., and I. F. A. Cavalcanti (2014), The relationship between the Antarctic oscillation and blocking events over the South Pacific and Atlantic Oceans, *Int. J. Climatol.*, *34*, 529–544, doi:10.1002/joc.3729.
Mendes, M. C. D., R. M. Trigo, I. F. A. Cavalcanti, and C. C. DaCamara (2008), Blocking episodes in the Southern Hemisphere: Impact on the climate of adjacent continental areas, *Pure Appl. Geophys.*, *165*, 1941–1962, doi:10.1007/s00024-008-0409-4.
Morgenstern, O., P. Braesicke, F. M. O'Connor, A. C. Bushell, C. E. Johnson, S. M. Osprey, and J. A. Pyle (2009), Evaluation of the new UKCA climate-composition model—Part 1 : The stratosphere, *Geosci. Model Dev.*, *2*, 43–57.
Morgenstern, O., G. Zeng, S. M. Dean, M. Joshi, N. L. Abraham, and A. Osprey (2014), Direct and ozone-mediated forcing of the Southern Annular Mode by greenhouse gases, *Geophys. Res. Lett.*, *41*, 1–8, doi:10.1002/2014GL062140.
Nishii, K., and H. Nakamura (2005), Upward and downward injection of Rossby wave activity across the tropopause: A new aspect of the troposphere–stratosphere dynamical linkage, *Q. J. R. Meteorolog. Soc.*, *131*, 544–563, doi:10.1256/qj.03.91.
Nishii, K., H. Nakamura, and Y. J. Orsolini (2011), Geographical dependence observed in blocking high influence on the stratospheric variability through enhancement and suppression of upward planetary-wave propagation, *J. Clim.*, *24*, 6408–6423, doi:10.1175/JCLI-D-10-05021.1.
Oberländer-Hayn, S., et al. (2016), Is the Brewer-Dobson circulation increasing or moving upward?, *Geophys. Res. Lett.*, *43*, 1772–1779, doi:10.1002/2015GL067545.
Oliveira, F. N. M., L. M. V. Carvalho, and T. Ambrizzi (2014), A new climatology for Southern Hemisphere blockings in the winter and the combined effect of ENSO and SAM phases, *Int. J. Climatol.*, *1692*, 1676–1692, doi:10.1002/joc.3795.
Parsons, S., J. A. Renwick, and A. J. McDonald (2016), An assessment of future Southern Hemisphere blocking using CMIP5 projections from four GCMs, *J. Clim.*, *29*, 7599–7611, doi:10.1175/JCLI-D-15-0754.1.
Pelly, J. L., and B. J. Hoskins (2003), A new perspective on blocking, *J. Atmos. Sci.*, *60*, 743–755, doi:10.1175/1520-0469(2003)060<0743:ANPOB>2.0.CO;2.
Pezza, A. B., P. van Rensch, and W. Cai (2012), Severe heat waves in Southern Australia: Synoptic climatology and large scale connections, *Clim. Dyn.*, *38*, 209–224, doi:10.1007/s00382-011-1016-2.
Pook, M. J., J. S. Risbey, P. C. McIntosh, C. C. Ummenhofer, A. G. Marshall, and G. A. Meyers (2013), The seasonal cycle of blocking and associated physical mechanisms in the Australian region and relationship with rainfall, *Mon. Weather Rev.*, *141*, 4534–4553, doi:10.1175/MWR-D-13-00040.1.
Renwick, J. A. (2005), Persistent positive anomalies in the Southern Hemisphere circulation, *Mon. Weather Rev.*, *133*, 977–988, doi:10.1175/MWR2900.1.
Rex, D. F. (1950), Blocking action in the middle troposphere and its effect upon regional climate. I. An aerological study of blocking action, *Tellus*, *2*, 196–211, doi:10.1111/j.2153-3490.1950.tb00331.x.
Risbey, J. S., M. J. Pook, P. C. McIntosh, M. C. Wheeler, and H. H. Hendon (2009), On the remote drivers of rainfall variability in Australia, *Mon. Weather Rev.*, *137*, 3233–3253, doi:10.1175/2009MWR2861.1.
Scaife, A. A., T. Woollings, J. Knight, G. Martin, and T. Hinton (2010), Atmospheric blocking and mean biases in climate models, *J. Clim.*, *23*, 6143–6152, doi:10.1175/2010JCLI3728.1.

Sinclair, M. R. (1996), A climatology of anticyclones and blocking for the Southern Hemisphere, *Mon. Weather Rev.*, *124*, 245–264, doi:10.1175/1520-0493(1996)124<0245:ACOAAB>2.0.CO;2.

Thompson, D. W. J., and J. M. Wallace (2000), Annular modes in the extratropical circulation. Part I: Month-to-month variability, *J. Clim.*, *13*, 1000–1016.

Thompson, D. W. J., M. P. Baldwin, and S. Solomon (2005), Stratosphere–troposphere coupling in the Southern Hemisphere, *J. Atmos. Sci.*, *62*, 708–715, doi:10.1175/JAS-3321.1.

Thompson, D. W. J., S. Solomon, P. J. Kushner, M. H. England, K. M. Grise, and D. J. Karoly (2011), Signatures of the Antarctic ozone hole in Southern Hemisphere surface climate change, *Nat. Geosci.*, *4*(11), 741–749, doi:10.1038/ngeo1296.

Tibaldi, S., and F. Molteni (1990), On the operational predictability of blocking, *Tellus A*, *42A*, 343–365, doi:10.3402/tellusa.v42i3.11882.

Trenberth, K. F., and K. C. Mo (1985), *Blocking in the Southern Hemisphere*, 3, vol. 113.

Wilcoxon, F. (1945), Individual comparisons by ranking methods, *Biom. Bull.*, *1*(6), 80–83.

WMO (2011), Scientific assessment of ozone depletion: 2010, *Tech. Rep. 52*, World Meteorological Organisation, Geneva, Switz.

Woollings, T., A. Charlton-Perez, S. Ineson, A. G. Marshall, and G. Masato (2010), Associations between stratospheric variability and tropospheric blocking, *J. Geophys. Res.*, *115*, 1–17, doi:10.1029/2009JD012742.

Yao, Y., and D. Luo (2015), Do European blocking events precede North Atlantic oscillation events?, *Adv. Atmos. Sci.*, *32*, 1106–1118, doi:10.1007/s00376-015-4209-5.1.